International Journal of Recent Technology and Engineering (IJRTE)
ISSN: 2277-3878, Volume-8 Issue-4, November 2019

State Dynamic Modeling using Ionic Conduction Phenomenon for TiO_2-based Memristive Thin Film

Raudah Abu Bakar, Nur Syahirah Kamarozaman, Wan Fazlida Hanim Abdullah, and Sukreen Hana Herman

Abstract*: *In this work a SPICE model was developed for metal-insulator-metal (MIM)-based memristors. The proposed model was achieved by combining the current conduction mechanisms with the dynamical state variable phenomenon. To account for ionic conduction in memristor, the Mott-Gurney law for ion hopping was incorporated in the state variable derivative. As compared to the experimental data, the proposed model is well matched with the measured data. The memristance and root mean square (RMS) error were calculated to be 120 Ω and 0.02 respectively. Simulating the proposed model at frequencies greater than unity formed a smaller hysteresis loop area.

Keywords* : *Titanium dioxide thin film, resistive switching, memristive behavior, SPICE model.

I. INTRODUCTION

Memristor is the fourth circuit element with the capabilities to memorize its present state during the removal of voltage [1], [2]. This two terminal device possesses a unique pinched hysteresis current-voltage (I-V) relationship, a Lissajous figure. Owing to its remarkable abilities and low power consumption due to its compact size, memristors have been extensively investigated to be potentially used in several applications including non-volatile memory, advanced computing system and sensor [3] – [6].

For the past few years, studies on memristor were focused on both the memristor fabrications [7] – [9] and the development of memristor model to predict the device performance at the circuit level in various applications [10] – [17]. In memristor modeling, the conduction mechanism and the dynamical phenomenon of state variable will be considered [2]. To date, the reported memristor SPICE models were ranging from linear [10], non-linear [11], tunnel-barrier [12], exponential [13] – [14] and physic-based memristor models [15] – [17]. Compared to all existing models, physic-based memristor model offers charge transport model for memristive devices due to the inclusion of ionic dynamical behavior in the state variable model. However, these models were used to describe the underlying dynamical switching behavior in tantalum oxide (TaO_x), tungsten oxide (WO) and chalcogenide-based memristor. Among the developed model, Amirsoleimani *et al*. proposed a physic-based model for titanium dioxide (TiO_2) thin film [17]. In this model the charge transport phenomenon was incorporated into the conduction mechanisms of Ag/TiO_2/ITO thin film. Although they could possibly predict and provide accurate model, different electrical and structural film character is the major limitation [17].

This work presents the development of SPICE model for TiO_2 thin film by combining the conduction mechanisms with the state variable. In order to account for dynamical phenomenon of oxygen vacancies in memristor, the Mott-Gurney law for ion hopping was employed. For further improvement, the threshold effect based on Yakopcic *et al*. was also incorporated into the model to include the non-linear dynamic effects in memristors [14]. The proposed model was then simulated using various types of input voltages and frequencies for validation.

II. CURRENT-VOLTAGE CHARACTERISTIC OF TiO_2-BASED MEMRISTIVE THIN FILM

Fig. 1(a) and (b) show the MIM memristive device structure consisted of platinum (Pt)/TiO_2/indium-doped tin oxide (ITO) substrate (Pt/TiO_2/ITO) and the device I-V characteristic respectively. The characteristic was obtained by applying the bias voltage on the top of Pt. The ITO substrate on the other hand served as the ground plane during the characterization process. The positive and negative voltages were applied to the MIM device. The current was then measured at the same time.

The memristive behavior of Lissajous pattern as shown in Fig. 1b was obtained after the I-V characterization of the TiO_2 thin film.

Manuscript published on November 30, 2019.
* Correspondence Author
Raudah Abu Bakar*, NANO-Electronic Centre (NET), Faculty of Electrical Engineering, Universiti Teknologi MARA, Shah Alam, Selangor Darul Ehsan, Malaysia, raudah088@uitm.edu.my.
Nur Syahirah Kamarozaman, NANO-Electronic Centre (NET), Faculty of Electrical Engineering, Universiti Teknologi MARA, Shah Alam, Selangor Darul Ehsan, Malaysia, nursyahirahk@uitm.edu.my.
Wan Fazlida Hanim Abdullah, Integrated Sensors Research Group, Universiti Teknologi MARA, Shah Alam, Selangor Darul Ehsan, Malaysia, wanfaz@uitm.edu.my.
Sukreen Hana Herman, Integrated Sensors Research Group, Universiti Teknologi MARA, Shah Alam, Selangor Darul Ehsan, Malaysia, hana1617@uitm.edu.my.

The I-V curve exhibit asymmetrical hysteresis loop characteristic. As suggested by A. Sawa, the observed phenomenon occurs on the account of the formation of the conducting path within the active layer formed after the I-V measurements [18]. The low (R_{ON}) and high (R_{OFF}) resistances were calculated to be 50 and 125 Ω respectively at 4.22 V as shown in Fig 1b. The detail fabrication method and results can be obtained from Kamarozaman *et al.* [19].

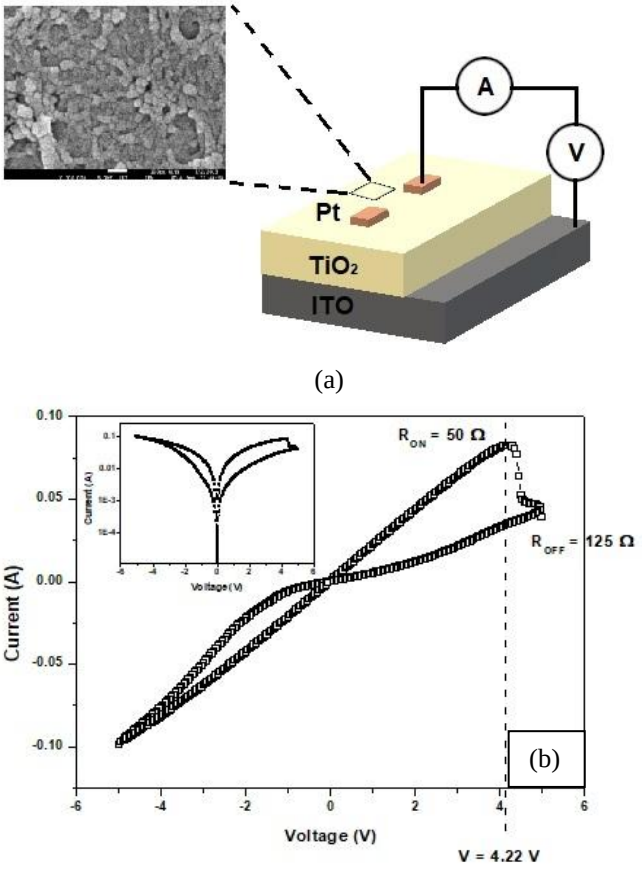

Fig. 1: (a) Schematic representation of TiO_2-based memristive device and the current-voltage characterization measurement setup. SEM micrographs of thin film after annealing process is also illustrated (Scale bar: 100 nm). (b) I-V characteristic of the MIM configuration showing the memristive behavior with the calculated R_{ON} and R_{OFF}. The upper inset shows the characteristic in logarithmic scale.

III. DEVICE MODEL

As proposed by Chua *et al.*, a memristive system can be generalized by a non-linear dynamical model as given by (1) and (2) respectively [2],

$$I(t) = g(w,t)V(t) \tag{1}$$

$$\frac{dw}{dt} = f(w(t)) \tag{2}$$

where, $I(t)$ and $V(t)$ are the output current and input voltage at time t, $g(w, t)$ is the conductance and w is the state variable for the memristive device respectively. The first equation basically described the conduction mechanism or current-voltage relationship of the device, whereas the dynamical evolution of the average oxygen vacancy concentration, w is given by the second equation.

The conduction mechanism of MIM structure was adopted from the previous study carried out by Chang *et al.*, and is given by the following equation [13],

$$I(t) = (1 - w(t))\alpha\left[1 - e^{-\beta V(t)}\right] + w(t)\gamma \sinh(\delta V(t)) \tag{3}$$

This model is developed based on the electrical properties at the electrode-insulator interface. As the work function of metal is differed from the metal oxide, the Schottky barrier is thus formed between the oxide thin film and ITO bottom electrode. Applying the positive voltage causes the positively charged oxygen vacancies to drift toward ITO substrate resulting in narrow Schottky barrier width. This will subsequently allow electrons to tunnel through the barrier and causing the tunneling current to be dominated. The application of negative voltage on the other hand, increases the width of the Schottky barrier. During this time the conduction is fully dominated by the Schottky current. According to equation (3), the conduction in memristor is dominated by Schottky mechanism if $w(t)$ is zero whereas the tunneling effect will become more apparent when $w(t)$ is unity.

The dynamical state variable is modeled by multiplying the $g(V(t))$ and $f(w(t))$ functions as given in equation (4) [14].

$$\frac{dw}{dt} = \eta(g(V(t))(f(w(t)) \tag{4}$$

The $g(V(t))$ is used to incorporate the threshold effect in the memristive device and is described by the following expression:

$$g(V(t)) = \begin{cases} A_p\left(e^{V(t)} - e^{V_p}\right), & V(t) > V_p \\ -A_n\left(e^{-V(t)} - e^{V_n}\right), & V(t) < -V_n \\ 0, & -V_n \le V(t) \le V_p \end{cases} \tag{5}$$

where, A_p and A_n are used to control the ionic speed and V_p and V_n represent the threshold voltage respectively. Whereas, $f(w(t))$ is used to model the dynamical ionic effects and is given by the following equation [20],

$$\frac{dw}{dt} = ace^{-\frac{U_a}{kT}} \sinh\frac{E}{E_o} \tag{6}$$

where a is the hopping distance, c is the escape-attempt frequency, U_a is the activation energy for migration, k is the Boltzmann's constant, T is the temperature in Kelvin, E is the electric field and Eo is expressed as

$$E_o = \frac{2kT}{qa} \tag{7}$$

IV. MEMRISTOR SPICE MODEL AND SIMULATION

As shown in Fig. 2, a memristive system for our proposed model was realized by combining two-terminal subcircuit blocks together. The first equivalent circuit (Fig. 2b), represents the current-voltage relationship between the top (TE) and bottom (BE) electrodes. The voltage controlled current sources Gm1 and Gm2 are used to model the Schottky and tunneling currents respectively.

Table I: The SPICE model subcircuit simulated in LTSPICE

```
* SPICE model for memristive devices
*
* Connections:
* TE - top electrode
* BE - bottom electrode
* SV - state variable
-------------------------------------------------------------------------------
* Fitting parameters to model different devices
* alpha, beta, gamma, delta: Fitting parameters to represent physical properties of material
* Vp, Vn: Pos. and neg. voltage thresholds
* Ap, An: Multiplier for SV motion intensity
* xp, xn: Points where SV motion is reduced
* xo: Initial value of SV
* eta: SV direction relative to voltage
* a: Hopping distance
* c: Attempt to escape frequency
* k: Boltzmann's constant
* T: Temperature
* q: Electronic charge
* Ua: Activation energy
* D: Device thickness
-------------------------------------------------------------------------------
1       .subckt mem_dev TE BE XSV

2       **Parameter values**
        .params Vp=4.25 Vn=1.0252 Ap=1.0894 An=0.0863 xp=0.9285 xn=0.6521
        +xo=0.0505 eta=0.6430 alpha=0.4153 beta=0.0545 gamma=0.5634 delta=0.0104
        +q=1.6021e-19 Ua=0.67 D=34.6e-9 a=1e-10 c=10e12 k=1.38e-23 T=300

3       **Function G(V(t)) - Describes the device threshold**
        .func G(V) { IF(V <= Vp, IF(V >= -Vn, 0, -An*(exp(-
        +V)-exp(Vn))), Ap*(exp(V)-exp(Vp)))}

4       **Function F(V(t),x(t)) - Describes the oxygen vacancies motion**
        .func F(V1,V2) { IF(eta*V1 >= 0, IF(V2 >= xp,
        +a*c*exp(-Ua/k*T)*sinh(q*a*abs(V1)/D*k*T)*wp(V2) ,1), IF(V2 <= (1-xn),
        +a*c*exp(-Ua/k*T)*sinh(q*a*abs(V1)/D*k*T)*wn(V2) ,1))}

5       **Window function**
        .func wp(V) { (xp-V)/(1-xp)+1}
        .func wn(V) { V/(1-xn)}

6       **Circuit to determine state variable**
        **dx/dt = F(V(t),x(t))*G(V(t))**
        .param cp={0.875}
        Cx XSV 0 {cp}
        .ic V(XSV) = xo
        Gx 0 XSV value={eta*F(V(TE,BE),V(XSV,0))*G(V(TE,BE))}

7       **Equation for Schottky current**
        Gm1 TE BE value ={(1-cp*V(XSV,0))*alpha*(1-exp(-beta*V(TE,BE)))}

8       **Equation for tunneling current**
        Gm2 TE BE value = {(cp*V(XSV,0))*gamma*sinh(delta*V(TE,BE))}

.ends mem_dev
```

Both current sources are connected in parallel between the TE and BE terminals. The second equivalent circuit (Fig. 2c) is responsible for the determination of the state variable. In this schematic diagram, a capacitor is connected in parallel with the current source, Gx. It is used for current integration purposes to produce the state variable.

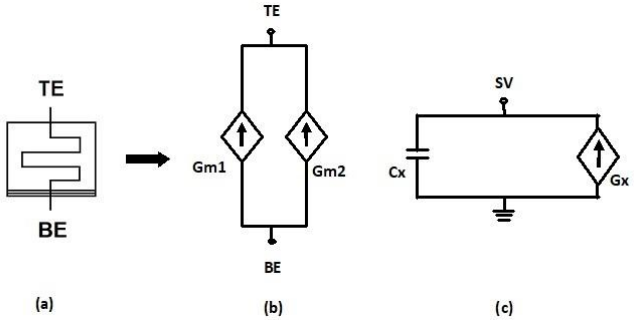

Fig. 2: (a) The symbol and the schematic diagrams of the SPICE model to represent (b) the current-voltage relationship between top (TE) and bottom (BE) electrodes and (c) state variable derivative at node SV.

Table I provides the memristive device subcircuit code used in the simulation using LTSPICE. In this netlist, it starts with parameter initialization. The parameters can be divided into constant values (e.g. Boltzmann's constant, electron charge and others), device based parameters (e.g. thickness) and fitting parameters (e.g. V_p, V_n, A_p, A_n and others). Line 3-5 specify the functions used to determine the device threshold, oxygen vacancies drift within the memristive device and window function respectively. Line 6 describes the equivalent circuit to determine the state variable (Fig. 2c). Lastly, the Schottky and tunneling currents that correspond to the equivalent circuit in Fig. 2b is given in line 7 and 8.

The simulation in the LTSPICE was performed by adjusting the fitting parameter values to obtain similar I-V characteristics as in Fig. 1b. In this simulation process, the direct current (DC) sweeps and sinusoidal input voltages were used. The RMS errors were calculated using

$$e_{v,i} = \sqrt{\frac{1}{N}\left(\frac{\sum_{n=1}^{N}\left(v_{s,n}-v_{r,n}\right)^2}{\bar{v}_r^{\,2}} + \frac{\sum_{n=1}^{N}\left(i_{s,n}-i_{r,n}\right)^2}{\bar{i}_r^{\,2}}\right)} \quad (7)$$

where $\bar{v}_r$, $\bar{i}_r$, v_s and i_s are the experimental and simulation voltage and current data, respectively [17]. Fig. 3 shows the circuit used in the LTSPICE for memristive device simulation process.

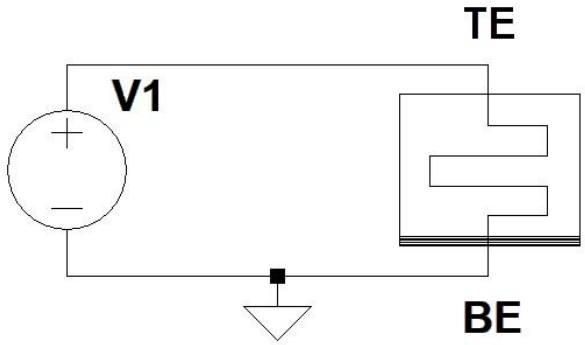

Fig. 3: Schematic diagram of memristive device for simulation process in LTSPICE where V1 is the input voltage (it can be either DC or sinusoidal input voltage).

V. SIMULATION OF THE PROPOSED MODEL

The simulation results using DC and sinusoidal input voltages were displayed in Fig. 4 and 5 respectively. The results showed that a well matched memristive behavior between the simulation results and experimental data were obtained. The RMS error using the DC input was calculated to be 0.02. Some discrepancies however observed during negative applied voltage for the simulation using sinusoidal input (Fig. 5a). The I-V characteristics in semi-logarithmic plots are shown in Fig. 4b and 5b. It is observed that the reset and set transitions were near the 4.35 and -5 V respectively for the simulation result and experimental data. It is thus suggested that the proposed SPICE model capable in capturing the reset and set processes precisely.

The simulated memristance values were 118 Ω and 109 Ω for DC and sinusoidal inputs respectively. The increases in the frequencies cause the shrink of the proposed model I-V characteristics as seen in Fig. 6.

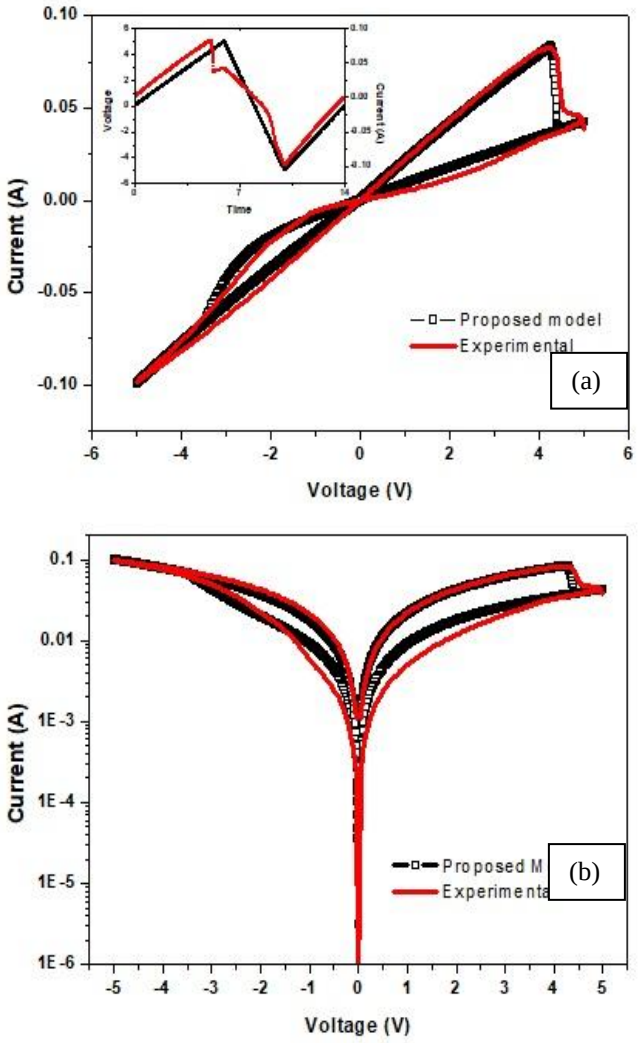

Fig. 4: The memristive behavior in (a) linear and (b) logarithmic plots. The upper insert displays the DC voltage input and the memristor current versus time respectively.

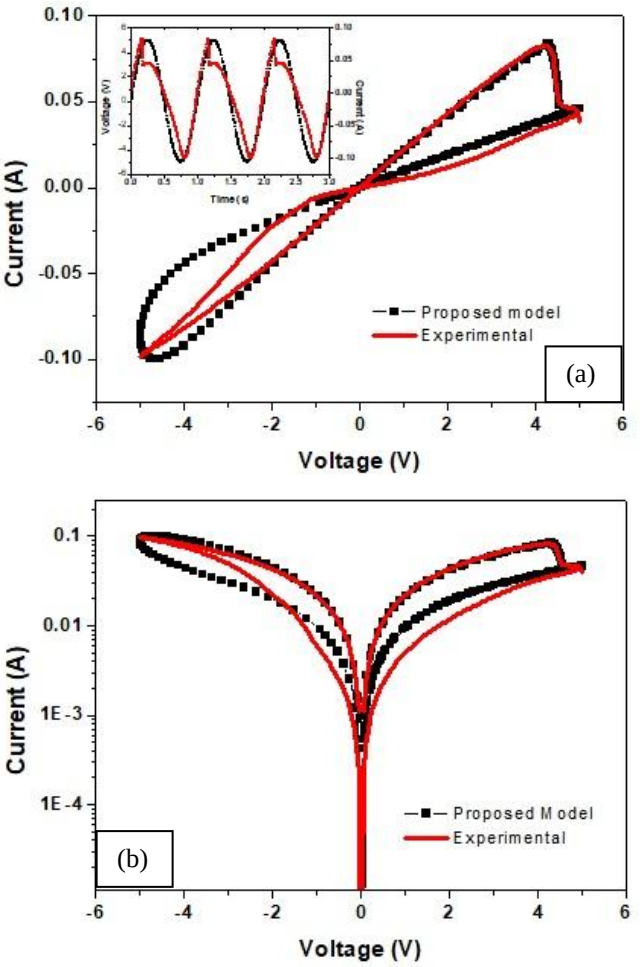

Fig. 5: The memristive behavior in (a) linear and (b) logarithmic plots. The upper insert displays the sinusoidal voltage input and the memristor current versus time respectively.

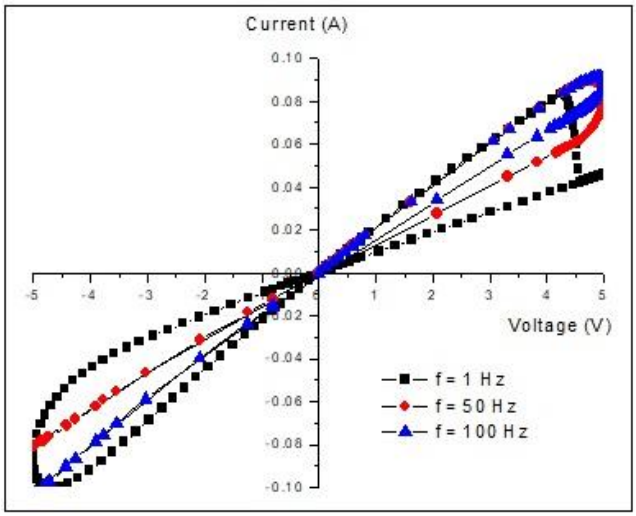

Fig. 6: I-V characteristics of the proposed model simulated at frequencies = 1, 50 and 100 Hz.

VI. CONCLUSION

In this work, a SPICE model was proposed for TiO_2-based memristive thin film. The model was developed by incorporating the dynamical ionic behavior into the Schottky and tunneling conduction mechanisms. The inclusion of ion hopping model resulted in a small RMS value. A shrinking of hysteresis loop was obtained as frequencies increase

ACKNOWLEDGMENT

A special thanks to all members of NANO-Electronic Centre (NET), Universiti Teknologi MARA, Malaysia for their help and support. Also to Institute of Research Management and Innovation (IRMI), Universiti Teknologi MARA, Malaysia. This work was funded by Ministry of Education Malaysia (MOE) under the Niche Research Grant Scheme (NRGS) (Project code: 600-RMI/NRGS 5/3 (7/2013)).

REFERENCES

1. R. S. Williams, "How we found the missing memristor," *IEEE Spectrum*, vol. 45, no.12, pp. 28-35, Dec. 2008.
2. L. O. Chua and S. M. Kang, "Memristive devices and systems," *Proc. IEEE*, vol. 64, pp. 209-223.
3. A. A. Haidrya, A. Ebach-Stahl and B. Saruhan, "Effect of Pt/TiO2 interface on room temperature hydrogen sensing performance of memristor type Pt/TiO_2/Pt structure", *Sensors and Actuators B*, 253, 2017, pp 1043–1054.
4. N. S. M. Hadis, A. A. Manaf, S. H. Ngalim and S. H. Herman, "Fabrication and characterisation of fluidic based memristor sensor for liquid with hydroxyl group", *Sensing and Bio-Sensing Research*, 14, 2017, pp. 21–29.
5. M. S. Feali, A. Ahmadi and M. Hayati, "Implementation of adaptive neuron based on memristor and memcapacitor emulators" *Neurocomputing*, 309, 2018, pp. 157–167.
6. K. Rajagopal, S. Kacar, Z.Wei, P. Duraisamy , T. Kifle and A. Karthikeyan, "Dynamical investigation and chaotic associated behaviors of memristor Chua's circuit with a non-ideal voltage-controlled memristor and its application to voice encryption", *Int. J. Electron. Commun. (AEÜ)*, 107, 2019, pp. 183–191
7. T.N.T.A. Aziz, A.B. Rosli, M.M. Yusoff, S.H. Herman, Z. Zulkifli, "Transparent hybrid ZnO-graphene film for high stability switching behavior of memristor device," *Mat. Sc. Semiconductor Processing*, Vol.89, January 2019, pp. 68-76.
8. Y. Yua, C. Wanga , C. Jianga, I. Abrahams, Z. Dua, Q. Zhang, J. Sun and X. Huang, "Resistive switching behavior in memristors with TiO2 nanorod arrays of different dimensions", *Applied Surface Science*, 485, 2019, pp. 222–229.
9. S. Hua, J. Yuea, C. Jianga, X. Tang, X. Huang, Z. Du and C. Wang, "Resistive switching behavior and mechanism in flexible TiO_2 memristor crossbars", *Ceramics International*, 45, 2019, pp. 10182–10186.
10. D. B. Strukov, G. S. Snider, D. R. Stewart and R. S. Williams, "The missing memristor found," *Nature*, vol. 453, no. 7191, pp. 80-83, May 2008.
11. J. Zha, H. Huang and Y. Lie, "A Novel Window Function for Memristor Model with Application in Programming Analog Circuits*," IEEE Trans. Ccts. Systems – II, Express Brief*, vol. 61, No. 5, 423-427, 2016.
12. H. Abdalla and M. D. Pickett, "SPICE modeling of memristors," *IEEE Int. Symp. Cct. Syst. (ISCAS)*, 2011, pp. 1832-1835.
13. T. Chang, S. S. H. Jo, K. H. Kim, P. Sheridan, S. Gaba S and Lu W, "Synaptic behaviors and modeling of metal oxide memristor device," *Appl Phys. A*, vol. 102, pp. 857-863, 2011.
14. C. Yakopcic, M. T. Taha, G. Subramanyam and R. E. Pino, "Memristor SPICE Model and Crossbar Simulation Based on Devices with Nanosecond Switching Time," *Int. Con. Neural Networks.*, 2013, pp. 464-470.
15. R. E. Pino, J. W. Bohl, N. McDonald, B. Wysocki, P. Rozwood, K. A. Campbell, A. Oblea and A. Timilsina, "Compact method for modeling and simulation of memristor devices: ion conductor chalcogenide-based memristor devices," *IEEE/ACM Int. Symp. Nanoscale Arch.*, 2010, pp. 1-4.
16. F. O. Hatem, T. N. Kumar and H. A. F. Almurib, "A SPICE Model of the Ta_2O_5/TaOx Bi-Layered RRAM", IEEE Trans. Circuits Syatems, Vol. 63, NO. 9, Sept. 2016, pp. 1487-1498
17. A. Amirsoleimani, J. Shamsi, M. Ahmadi, A. Ahamdi, S. Alirezaee, K. Mohammadi, M. A. Karami, C. Yakopcic, O. Kavehei and S. Al-Sarawi, "Accurate charge transport model for nanoionic memristive devices," *Microelectr. J.*, vol. 65, pp. 49-57, 2017.
18. A. Sawa, "Resistive switching in transition metal oxides," *Mat. Today*, Vol. 11, pp. 28-36, 2008.
19. N. S. Kamarozaman, M. F. Mohamed Soder, M. Z. Musa, R. A. Bakar, W. F. H. Abdullah, S. H. Herman and M. Rusop, "Effect of post-deposition annealing process on the resistive switching behavior of TiO_2 thin films by sol-gel method," *Adv-Maters. Research.*, vol. 925, pp. 125-129, 2014.
20. F. Hossein-Babaei and N. Alaei-Sheini, "Electronic Conduction in Ti/Poly-TiO_2/Ti Structures," *Sci. Rep.*, vol. 6, 2016.

AUTHORS PROFILE

Raudah Abu Bakar received her B. Eng and M. Sc degrees from University of Surrey (2002) and Universiti Teknologi MARA (2008) respectively. She is now working towards her Ph.D. degree in Universiti Teknologi MARA.

Nur Syahirah Kamarozaman is a lecturer in Faculty of Electrical Engineering, Universiti Teknologi MARA, Terengganu Campus, Malaysia. Her B. Eng (Hons.) and M. Sc degree in Science Electrical Engineering were awarded from the Universiti Teknologi MARA Malaysia in 2011 and 2015 respectively.

Wan Fazlida Hanim Abdullah received her B.Eng (Hons) Electronics Engineering from University of Southampton (1993), MSc in electronic engineering from Universiti Putra Malaysia (2002) and PhD in Microengineering and Nanoelectronics from Universiti Kebangsaan Malaysia (2010). She is interested in microelectronic devices, solid-state sensors, nanoelectronics and sensor interfacing circuits researches. Her current projects are extended-gate field-effect transistor sensor readout circuitry, multisensory environment with data analytics and ROICs for amperometric DNA biosensors. She is now an Assistant Professor in the Faculty of Electrical Engineering, Universiti Teknologi MARA, Malaysia.

Sukreen Hana Herman is the head of the Integrated Sensor Research group in the Faculty of Electrical Engineering, UiTM. Her B.Eng degree in Electrical, Electronics and Information engineering and M.Eng in Electronics and Computer Science were awarded by the Kanazawa University, Japan in 1999 and 2004, respectively while her PhD in Materials Science in 2009 from the Japan Andvanced Institute of Science and Technology (JAIST). She is interested in conducting the researches in fabrication and characterization of semiconductor materials, sensing membranes and nanostructured materials. She is one of the authors for numbers of articles and conference proceedings and has received various major awards in invention and innovation exhibition and competitions.